Title
THE MORPHOLOGICAL STABILITY OF CONTINUOUS INTERGRANULAR PHASES

Authors
Carter, W.C.
Glaeser, A.M.

Publication Date
1985-07-01

Lawrence Berkeley Laboratory
UNIVERSITY OF CALIFORNIA

Materials & Molecular Research Division

Presented at the Twenty-First University Conference on Ceramic Science, University Park, PA, July 17-19, 1985; and to be published in the Proceedings

THE MORPHOLOGICAL STABILITY OF CONTINUOUS INTERGRANULAR PHASES

W.C. Carter and A.M. Glaeser

July 1985

Prepared for the U.S. Department of Energy under Contract DE-AC03-76SF00098

DISCLAIMER

LBL-19160

To be published in: Proceedings of the Twenty-First University Conference on Ceramic Science, Penn State University, July 17-19, 1985.

The Morphological Stability of Continuous Intergranular Phases

by

W. Craig Carter and Andreas M. Glaeser

Department of Materials Science
and Mineral Engineering, and
Materials and Molecular Research Division
Lawrence Berkeley Laboratory
University of California
Berkeley, California 94720

ABSTRACT:

A thermodynamic analysis of the morphological stability of continuous intergranular phases, incorporating the number of bounding grains **n**, and dihedral angle ψ as variables is presented. For each **n**, the minimum thermodynamically unstable wavelength of an infinitesimal amplitude perturbation coincides with the Rayleigh result for $\psi = 180°$, increases with decreasing ψ and tends to infinity as ψ approaches $\pi - (2\pi/n)$, or equivalently as the interface curvature vanishes. For fixed ψ, the stability increases with **n**. Several applications and implications of the analysis are discussed.

This work was supported by the Director, Office of Energy Research, Office of Basic Energy Sciences, Materials Sciences Division of the U.S. Department of Energy under Contract No. DE-AC03-76SF00098.

1. INTRODUCTION:

The morphological instability of continuous phases has received considerable attention subsequent to the first complete analysis of such phenomena by Rayleigh[1] in 1878. As Rayleigh remarked, "[these] phenomena, interesting not only in themselves, but also as throwing light upon others yet more obscure, depend for their explanation upon the transformations undergone by a [cylindrical body] when slightly displaced from its equilibrium configuration and left to itself."[2] The well known result of the Rayleigh analysis is that any infinitesimal periodic perturbation with a wavelength exceeding the (cylinder) circumference will increase in amplitude, and eventually cause the formation of one discrete particle for each wavelength increment of cylinder.

The Rayleigh analysis has been applied to a number of microstructural phenomena involving capillarity-induced shape changes. Among these are: the stability of lamellar eutectics[3], fibers in composites[4], artificially lengthened precipitates[5,6], shape evolution of field ion emitter tips[7,8], healing of cracks introduced by thermal shock[9], as well as by scoring and welding of bicrystals[10,11], and the stability of the continuous pore phase during sintering of powder compacts.[12,13]

While in some of the aforementioned applications the Rayleigh analysis may be valid, complications arise when the continuous phase is located at a grain boundary. For an intergranular phase, each grain boundary intersection is characterized by some dihedral angle.

C. S. Smith was perhaps first to recognize the modifying effect of dihedral angle on the stability of continuous grain boundary phases.[14]

In discussing continuous phases along three grain junctions Smith wrote, "If a second phase forming at a grain edge has a dihedral angle against grain boundaries of nearly 180°, it will behave like a cylinder and will certainly break up. If, however, the interphase tension is low in comparison with the adjacent grain boundary tension, the resulting triangular shape becomes stable at longer and longer lengths until, at a dihedral angle of 60° and below, the phase becomes stable at any length of grain edge.".

Continuous phases may be situated at (along) the junctions of an arbitrary number of grains. The analysis presented, quantifies the discussion of Smith by extending the method of Rayleigh to geometries of continuous phases surrounded by **n** grains with (variable) dihedral angle ψ. Results indicate the stability condition depends strongly on the intergranular phase geometry, and may differ significantly from that of a cylinder.

A complete analysis of morphological instability consists of two parts[15]: a thermodynamic analysis identifying the smallest wavelength (infinitesimal amplitude) perturbation for which the amplitude will increase, and a kinetic analysis determining the particular wavelength for which perturbation growth is most rapid. In this paper, we present a thermodynamic analysis for nonfaceting surfaces with single-valued interfacial tensions. Possible modifications which may result from surface faceting, as well as the implications of the analysis to the kinetics of phase breakdown are qualitatively addressed. A kinetic analysis is forthcoming.[16]

2. THEORETICAL ANALYSIS: DETERMINATION OF λ_{min}

The ensuing sections describe the assumptions made and procedures used in the analysis. The objectives are the calculation of the surface area and volume of both a perturbed and an unperturbed channel as a function of the number of bounding grains **n**, and the dihedral angle ψ. The results of these calculations are employed to define the condition for thermodynamic stability of a continuous grain boundary phase.

2.1 Geometry

Figure 1 illustrates most of the geometrical parameters relevant to the analysis. When the intersection points of the intergranular phase with the n grain boundaries are joined by straight line segments, an n-sided polygon is produced. When the surface energy is isotropic, equilibrium requires the curvature of each bounding interface be constant. If the surface energy of the n interfaces is identical, the polygon will display n-fold symmetry.

The polygon is circumscribed by a circle of radius R_c. Each interface may be described by a circle of radius ρ. It is always possible to pick one circle of radius ρ such that its center coincides with the Cartesian origin. Requiring the interfaces to have a common dihedral angle ψ leads to

$$\frac{\rho}{\sin(\pi/n)} = \frac{-R_c}{\cos(\psi/2 + \pi/n)} \qquad (1)$$

A perturbation on the radius of curvature can be described as the largest term of some periodic function, i.e.,

$$\rho = \rho_o + \delta \cos kz \tag{2}$$

where $k = 2\pi/\lambda$, z is the axial (longitudinal) coordinate of the cylinder, and δ an arbitrarily small amplitude.

2.2 Determination of Surface Area

The grain boundary area per wavelength perturbation is

$$A_{gb} = n \int_0^{2\pi/k} (\alpha - R_c)\, dz \tag{3}$$

$$= n \int_0^{2\pi/k} \alpha + (\rho_o + \delta \cos kz) \frac{(\cos(\psi/2 + \pi/n))}{\sin(\pi/n)}\, dz \tag{4}$$

$$= \frac{2n\pi\alpha}{k} + \frac{2n\pi\rho_o}{k} \frac{\cos(\psi/2 + \pi/n)}{\sin(\pi/n)} \tag{5}$$

where α is some arbitrary length.

The superficial area per wavelength perturbation is (in cylindrical coordinates)

$$A_s = n \int_{-\beta}^{\beta} d\theta \int_0^{2\pi/k} dz\, \rho\, (1 + (d\rho/dz)^2)^{\frac{1}{2}} \tag{6}$$

where

$$\beta = \psi/2 + \pi/n - \pi/2 \tag{7}$$

Since $d\rho/dz$ is of order δ and arbitrarily small,

$$A_s \simeq 2n \int_0^{\beta} d\theta \int_0^{2\pi/k} dz \, (\rho_o + \delta \cos kz) \left(1 + \frac{\delta^2 k^2 \sin^2 kz}{2}\right) \quad (8)$$

$$= \frac{4n\pi\rho_o}{k} \left(1 + \frac{\delta^2 k^2}{4}\right) \beta \quad (9)$$

2.3 Volume Determination and Criterion for Break-up

The cross-sectional area of the intergranular phase (channel) is

$$A_{cs} = n\rho^2(\beta + [\sin^2\beta \cos(\pi/n)/\sin(\pi/n)] - \sin\beta \cos\beta) \quad (10)$$

$$= n\rho^2\chi \quad (11)$$

The channel volume per perturbation wavelength is

$$V = \frac{2n\pi\chi}{k} (\rho_o^2 + \delta^2/2) \quad (12)$$

which yields

$$\rho_o^2 = \xi^2 (1 + (\delta^2/2\xi^2)) \quad (13)$$

where

$$\xi^2 = kV/2n\pi\chi \quad (14)$$

To sufficient approximation

$$\rho_o = \xi (1 - (\delta^2/4\xi^2)) \quad (15)$$

Defining the surface energy $\gamma_s = 1$, then $\gamma_{gb} = 2 \cos \psi/2$. The superficial energy per wavelength is

$$\Gamma = A_s + 2 \cos(\psi/2) \; A_{gb} \tag{16}$$

$$= \frac{4n\pi\rho_o}{k}(1 + \frac{\delta^2 k^2}{4})\beta + \frac{4n\pi\rho_o}{k}\frac{\cos(\psi/2 + \pi/n)\cos\psi/2}{\sin\pi/n}$$

$$+ \frac{4n\pi\alpha\cos\psi/2}{k} \tag{17}$$

Using Eq. 15 yields

$$\Gamma = \frac{4n\pi\xi}{k}(\beta + \frac{\cos(\psi/2 + \pi/n)\cos\psi/2}{\sin\pi/n}) + \frac{4n\pi\alpha\cos\psi/2}{k}$$

$$+ \frac{n\pi\beta\delta^2}{k\xi}[(k^2\xi^2 - \frac{(1 + \cos(\psi/2 + \pi/n)\cos\psi/2)}{\beta\sin\pi/n}] \tag{18}$$

Eq. 18 is equivalent to an expansion of the surface energy per wavelength about the radius ρ_o

$$\Gamma(\rho) = \Gamma(\rho_o) + \Gamma'(\rho_o)\int_0^{2\pi/k}(\rho - \rho_o)dz$$

$$+ \Gamma''(\rho_o)\int_0^{2\pi/k}\tfrac{1}{2}(\rho - \rho_o)^2 dz \tag{19}$$

$$= \Gamma(\rho_o) + \Gamma''(\rho_o)(\pi\delta^2/2k) + \ldots \tag{20}$$

As in all metastability problems, the stability depends on the sign of Γ''. It is sufficient to approximate

$$\rho^2 = \xi^2 \tag{21}$$

when establishing the sign of Γ''.

The growth of any perturbation of wavelength $\lambda > \lambda_{min}^{\cdot}$ is energetically favorable where

$$\frac{\lambda_{min}}{2\pi\rho} = \left(1 + \frac{\cos(\psi/2 + \pi/n)\cos\psi/2}{\beta \sin \pi/n}\right)^{-\frac{1}{2}} \qquad (22)$$

which may be written more simply as

$$\frac{\lambda_{min}}{2\pi\rho} = \left(\frac{\beta}{\chi}\right)^{\frac{1}{2}} \qquad (23)$$

or in terms of the convenient R_c

$$\frac{\lambda_{min}}{2\pi R_c} = \left(\frac{\beta}{\chi}\right)^{\frac{1}{2}} \frac{\sin \pi/n}{\sin \beta} \qquad (24)$$

3. DISCUSSION:

Results of the analysis for several **n** are illustrated in Figure 2. For each **n**, the minimum thermodynamically unstable infinitesimal wavelength perturbation wavelength coincides with the Rayleigh result for $\psi = 180°$, increases with decreasing ψ, and tends to infinity as ψ approaches $\pi - (2\pi/n)$, or equivalently, as the interface curvature vanishes. For fixed **n**, a continuous phase with lower ψ is expected to be more stable than one with higher ψ. The phase is completely stable to perturbations when $\psi \leq \pi - (\pi/2n)$. For fixed ψ, the stability increases with **n** (Table I).

To facilitate comparison between this analysis and that of Rayleigh, a normalization parameter is introduced. Defining R_{eq} as the radius of a cylinder having the same volume per unit length as an intergranular phase characterized by a dihedral angle ψ, the ratio $\lambda_{min}/2\pi R_{eq}$ normalizes the actual λ_{min} by the minimum wavelength that

would grow in a geometrically similar compact with an equivalent volume fraction of second phase. The dependence of $\lambda_{min}/2\pi R_{eq}$ on **n** for $\psi = 145°$ is presented in Table I.

3.1 General Considerations:

The nature of a second phase, its composition, inherent properties, morphology, and distribution within a matrix, can have an important bearing on a material's ultimate properties. Introduction of continuous filaments into polycrystalline matrices may dramatically alter mechanical behavior. High temperature stability and useful lifetimes of such composites will be influenced by the fibers' stability against breakdown. Continuous phases may provide high diffusivity transport paths, or be preferentially leached, thus limiting the utility of a material in storage applications, e.g., containment of nuclear waste. In these cases as well as others, factors influencing the morphological stability of continuous phases may become important elements in materials design. In the following, a number of specific cases are considered, and the extent to which dihedral angle may stabilize an intergranular phase is indicated.

3.2 Consideration of n = 2

The dihedral angle, through its effect on λ_{min} will affect both the size and spacing of discrete particles or phases produced by perturbation growth processes. Experiments conducted on bicrystals with a systematic variation in ψ (misorientation) would be expected to reveal a systematic variation in particle size and spacing. In polycrystals

with a spectrum of ψ, "scatter" in the sizes and spacings of discrete particles would be expected.

Numerous experiments have investigated the healing of intergranular cracks. High aspect ratio intergranular pore channels have been introduced by scoring and welding bicrystals[10,11], as well as by thermal shock of polycrystals.[9] Micrographic evidence indicates that pore breakup during subsequent annealing is somewhat erratic, i.e., the wavelength of breakup appears to vary from one channel to the next. This may in large part reflect differences in pore channel size. In addition however, results presented by Gupta for alumina[9], indicate the final pore spacing to pore radius **ratio** may vary by as much as factor two*.

One expects the morphological evolution of these systems to be affected by the presence of grain boundaries. A factor two variation in pore spacing:pore radius ratio, if entirely due to variations in λ, would require λ to vary by a factor ≈ 3. Although dihedral angles were not measured in the studies cited, recent dihedral angle measurements in alumina by Handwerker[18] have indicated a wide dihedral angle range, 85° to 170°. This range of ψ, would lead to a factor ≈ 2.5 variation in λ_{min}, and must similarly affect the kinetically dominant wavelength. As discussed in Section 3.5, such shifts in pore spacing:pore radius ratios may have an important effect on the magnitude of transport coefficients deduced from such experiments.

---

*Although the center to center pore spacing in a 2-D projection permits an assessment of the perturbation **wavelength**, it is not possible to assess the ratios $\lambda_{min}/2\pi R_{eq}$ or $\lambda_{min}/2\pi\rho$ without dihedral angle measurements.

3.2 Consideration of n = 3

During intermediate stage sintering, the pore phase is often approximated as a cylindrical channel along three grain junctions. Breakdown of the continuous pore phase, marking the transition from intermediate to final stage sintering has been assumed to occur by perturbation growth processes. Recently, micrographic evidence was obtained suggesting a Rayleigh instability of pore channels along three-grain junctions.[13] The results of the present analysis, as well as inconsistencies between observed behavior and kinetic behavior predicted for cylinders, suggest breakdown of the pore phase may be significantly more complex than previously assumed.

The pore cross-section in an unfired compact comprised of spherical particles is nonuniform. Neck growth associated with densification would be expected to lead to pore channel closure at the point of initial minimum cross-section, the three grain junction midpoint. However, if the initial perturbation is unstable and mass redistribution along the pore channel is rapid in comparison to channel shrinkage, perturbation decay, followed by channel shrinkage and ultimately, pore closure due to the growth of morphological perturbations may become possible.

Dihedral angle will affect the driving force for perturbation growth and densification. As ψ is decreased, the driving force for perturbation growth decreases if $\lambda_{initial} > \lambda_{min}$; the driving force for decay is increased when $\lambda_{initial} < \lambda_{min}$. A decrease in ψ decreases the driving force for densification. Thus, in systems with low ψ and/or high surface diffusivities or vapor pressures, perturbation decay is favored. After sufficient channel shrinkage to support perturbation

growth along a facet length channel, a Rayleigh instability may ensue, leading to formation of closed pores along three-grain junctions and at four grain junctions. In contrast, in systems with high ψ and high grain boundary or lattice diffusivities, growth of the initial perturbation may be energetically favorable, or channel shrinkage may occur more rapidly than perturbation decay. Both situations will lead to the development of isolated pores at four-grain junctions only. Resulting differences in pore volume and location will effect the pore mobility, and thus mechanisms and conditions for pore-grain boundary separation.

The dihedral angle distribution may have an important modifying effect on microstructural evolution. In materials with a broad dihedral angle distribution, the processes dominating the pore phase's morphological evolution may vary within a compact, resulting in a spectrum of pore-grain boundary separation conditions. This factor, combined with effects of ψ on pore shrinkage and coarsening behavior, as well as pore mobility[17], may contribute to the development of microstructural inhomogeneities promoting the initiation of abnormal grain growth.

Narrowing the dihedral angle distribution would be expected to lead to more uniform microstructure development. A comparison of dihedral angle measurements in undoped and MgO-doped Al_2O_3[18], has indicated that dopant additions reduce the width of the dihedral angle distribution. Handwerker et al. point out this increases the uniformity of microstructural evolution by reducing the variation in driving forces for densification.[19] The potential benefits of a dopant-induced reduction in boundary mobility have frequently been cited. Dopant

effects on the uniformity of the pore structure produced during the transition from intermediate to final stage sintering may also be important.

In addition to the pore phase in powder compacts, second phases at three-grain junctions are commonly found in alloys with a large difference in either the melting points or solubilities of the constituents.[14] A residual glassy phase along three-grain junctions may also develop in liquid-phase sintered materials. Similar stabilizing effects may be of importance in these cases as well.

3.3 Consideration of $n \geq 4$

Table I illustrates the pronounced increase in stability to perturbation growth accompanying an increase in **n** (ψ constant). The enhanced stability is manifested in two ways. The stabilizing effect becomes significant at progressively higher ψ as **n** increases, and the dihedral angle range within which perturbation growth is possible diminishes (Figure 2). Thus stabilization effects of the type considered are expected to be extremely important when a continuous phase is bounded by a large number of grains.

High coordination number stacking faults in wire sintering experiments would be expected to be extremely stable to perturbation growth. Similar effects may also be important for stacking faults in conventional powder compacts. The high temperature stability of fibers in composites is expected to be affected by the values of ψ and **n**. Subject to other constraints, it would be advantageous to maximize the number of coordinating grains. Thus grain size:fiber diameter ratio (Q) emerges as a potentially important parameter in materials design.

Grain growth and fiber coarsening may modify **n**, introducing an additional time-dependent component to morphological stability. Grain growth may dramatically decrease fiber stability within certain ranges of **Q**. A decrease in **Q** from 20 to 4 may only have a limited effect, whereas an additional factor of 2-3 increase in grain size would likely have a profound influence on fiber stability. High temperature stability of properties may increase from use of grain growth inhibitors during materials fabrication.

When **n** is sufficiently large to inhibit perturbation growth processes, other factors inducing mass redistribution along fibers may assume greater significance. A "perturbation" or variation in the number of coordinating grains along the fiber axis will produce local curvature differences may may induce mass transfer from regions of lower n to higher-n regions. Thus, relatively coarse-grained regions may emerge as preferential fiber-pinchoff sites. Microstructural homogeneity thus becomes an issue of considerable importance.

3.4 Anisotropic Interfacial Energies

Isotropic surface energies have been assumed, however, both grain boundary and surface energies may vary within an individual channel. This anisotropy may introduce both variable surface curvature and variable dihedral angles. Geometric modelling of this situation is tedious but not difficult: metastable configurations can be determined.*

---

*It is interesting to note that if all bounding surfaces are comprised of the same phase, metastability requires that all bounding segments have nonzero curvature or that all have zero curvature. Thus,
(Footnote Continued)

However, each case is unique, and therefore, the problem is not amenable to generalization.

Facetting presents an additional complication. Cahn has evaluated the stability of single crystal rods with a specific surface energy isotropic in transverse planes, but a function of $\phi = (\partial R/\partial z)$.[20] Surface energy anisotropy may have either a stabilizing or destabilizing effect, depending on the manner in which γ varies with surface reorientation. If the original surface orientation corresponds to a cusp in the γ versus ϕ plot, the cylinder is stabilized with respect to infinitesimal perturbations, however, may be unstable to finite perturbations. In contrast, when the original surface corresponds to a ridge in the γ - ϕ plot, the cylinder is unstable. More generally, λ_{min} depends on the second derivative of γ with respect to ϕ. If $(\partial^2\gamma/\partial\phi^2)$ is positive (corresponding to minimum in γ at $\phi = 0$), λ_{min} is increased, and conversely.

Although similar behavioral trends might be anticipated for intergranular phases, inclusion of torque terms reflecting the orientation dependence of interfacial energies into an analysis appropriate to intergranular phases would be more difficult, and introduce numerous complications. Even if the continuous phase is a single crystal, there will be n distinct misorientations and hence interphase boundaries for an n-grain coordinated phase at each location along the z-axis. Conceivably, the interface orientation of one interphase boundary lies near a cusp orientation, while the adjacent

---

(Footnote Continued)
the analysis is not applicable to situations where only one bounding surface has zero curvature.

interphase boundary lies in a position corresponding to a ridge in the γ - ϕ plot. Consequently, quantitative assessment of surface energy anisotropy effects is a formidable task.

3.5 Kinetic Implications

The stability condition defined is thermodynamic; if any mass transport systems are operative that permit the development and growth of perturbations, equilibrium will be established by growth of a perturbation with $\lambda > \lambda_{min}$. For intergranular phases, λ_{min}, and thus the kinetically favored wavelength will depend on both ψ and **n**.

Kinetic models predict the rate at which equilibrium will be established, and the perturbation wavelength which maximizes the driving force:transport distance ratio. For a cylindrical void with isotropic interfacial energy, both the perturbation growth rate and magnitude of the kinetically dominant wavelength are predicted to depend on the dominant mass transport system.[7] An analysis by Nichols and Mullins suggests the most rapidly growing wavelength will vary from $\sqrt{2}\cdot\lambda_{min}$ for surface diffusion dominated growth to $2.1\lambda_{min}$ for volume diffusion dominated growth. Intermediate values are predicted when both mechanisms contribute substantially to breakdown.

Qualitatively similar behavior is anticipated for breakdown of continuous intergranular phases. However, in such cases, ψ and **n** will have a modifying influence. Since the most rapidly growing wavelength must exceed λ_{min}, the kinetically dominant wavelength must also vary with ψ. One anticipates rates of evolution become vanishingly low as ψ approaches $\pi - (2\pi/n)$, since the chemical potential gradient must vary at least linearly with the inverse of the dominant wavelength.

The dihedral angle and number of bounding grains will affect both the spacing and size of discrete "particles" or phases produced by perturbation growth processes. Since these parameters are used to both identify the dominant transport mechanism and estimate the magnitude of the appropriate transport coefficient, application of kinetic analyses appropriate to cylinders to the breakdown of intergranular phases, without consideration of dihedral angle effects, may introduce systematic errors.[16] Plausibly, transport coefficients determined in this way may be in error, and/or differ considerably from those determined using other methods.

3.6 Cautions and Limitations

The stability condition derived in this analysis defines the minimum wavelength necessary for a **sinusoidal** perturbation to increase in amplitude. As detailed in Section 2, sinusoidal perturbations with $\lambda > \lambda_{min}$ decrease the surface area per wavelength perturbation, and thus decrease the surface energy in comparison to that of an unperturbed cylinder having the same volume per wavelength.

The surface area of the perturbed "cylinder" is obviously sensitive to the form of the imposed perturbation. Thus, it is conceivable that a perturbation with an additional radial or rotational component could yield a λ_{min} smaller than that derived here. Hence, although the calculated values for λ_{min} presented serve as a **sufficient** condition for instability, it is necessary to acknowledge the possibility that perturbations of more complex geometry may provide a different and smaller value for λ_{min} as a **necessary** condition for instability.

Acknowledgements:

This work was supported by the Office of Energy Research, Office of Basic Energy Sciences, Materials Sciences Division of the U. S. Department of Energy under Contract No. DE-AC03-76SF00098. One of the authors (WCC) was supported in part by an ARCO Foundation Fellowship. Rowland M. Cannon, Lorenzo Sadun and John Salmon are thanked for helpful discussions and comments. Finally, we wish to acknowledge the enthusiastic support of G. O. Bears.

References:

1. Lord Rayleigh, "On the Instability of Jets," Proc. London Math. Soc., 10, 4-13 (1879).

2. Lord Rayleigh, Theory of Sound, Vol. 2, 2nd Edition, MacMillan and Co., London, (1929).

3. H. E. Cline, "Shape Instabilities of Eutectic Composites at Elevated Temperatures," Acta Metall., 19, [6], 481-90 (1971).

4. A. J. Stapley and C. J. Beevers, "The stability of sapphire whiskers in nickel at elevated temperatures, Part 2," J. Mater. Sci., 8, 1296-1306 (1973).

5. M. McLean, "The kinetics of spheroidization of lead inclusions in aluminium," Philos. Mag., 27, 1253-66 (1973).

6. D. M. Moon and R. C. Koo, "Mechanism and Kinetics of Bubble Formation in Doped Tungsten," Met. Trans., 2, [8], 2115-22 (1971).

7. F. A. Nichols and W. W. Mullins, "Surface (Interface) and Volume-Diffusion Contributions to Morphological Changes Driven by Capillarity," Trans. A.I.M.E., 233, [10], 1840-48 (1965).

8. F. A. Nichols and W. W. Mullins, "Morphological Changes of a Surface of Revolution due to Capillarity-Induced Surface Diffusion," J. Appl. Phys., 36, [6], 1826-35 (1965).

9. T. K. Gupta, "Instability of Cylindrical Voids in Alumina," J. Am. Ceram. Soc., 61, [5-6], 191-95 (1978).

10. C. F. Yen and R. L. Coble, "Spheroidization of Tubular Voids in Al_2O_3 Crystals at High Temperatures," ibid., 55, [10], 507-09 (1972).

11. O. Maruyama and W. Komatsu, "Observations on the Grain-Boundary of Al_2O_3 Bicrystals," Ceramurgica International, 5, [2], 51-5 (1979).

12. W. C. Carter and A. M. Glaeser, "Dihedral Angle Effects on the Stability of Pore Channels," J. Am. Ceram. Soc., 67, [6], C124-C127 (1984).

13. M. D. Drory and A. M. Glaeser, "The Stability of Pore Channels: Experimental Observations," ibid., 68, [1], C14-C15 (1985).

14. C. S. Smith, "Grains, Phases, and Interfaces: An Interpretation of Microstructure," Trans. A.I.M.E., 175, [1], 15-51 (1948).

15. F. A. Nichols, "On the Spheroidization of Rod-Shaped Particles of Finite Length," J. Mater. Sci., 11, [6], 1077-82 (1976).

16. W. C. Carter and A. M. Glaeser, to be published

17. C. H. Hsueh, A. G. Evans, and R. L. Coble, "Microstructure Development During Final/Intermediate Stage Sintering - I. Pore/Grain Boundary Separation," Acta Metall., 30, [7], 1269-79 (1982).

18. C. A. Handwerker, "Sintering and Grain Growth in MgO"; Sc.D. Thesis, Massachusetts Institute of Technology, Cambridge, MA, February 1983.

19. C. A. Handwerker, R. M. Cannon, and R. L. Coble, "Final Stage Sintering of MgO," pp. 619-43 in Structure and Properties of MgO and Al_2O_3 Ceramics, Vol. 12 in Advances in Ceramics, W. D. Kingery, Ed., ACS Publication (1984).

20. J. W. Cahn, "Stability of Rods with Anisotropic Surface Free Energy," Scripta Metall., 13, [11], 1069-71 (1979).

Figure Captions:

Figure 1 Geometry of intergranular phase, and illustration of parameters ρ, R_c, and dihedral angle ψ.

Figure 2 Ilustration of effect of varying **n** and ψ on the stability of continuous intergranular phases.

Table Captions:

Table I Comparison of $\lambda/2\pi R_c$, $\lambda/2\pi\rho$, and $\lambda/2\pi R_{eq}$ for $\psi = 145°$ and n varying from 2 to 11.

Table I

$\psi = 145°$

n	$\lambda_{min}/2\pi R_c$	$\lambda_{min}/2\pi\rho$	$\lambda_{min}/2\pi R_{eq}$
2	1.19	1.14	1.44
3	1.55	1.21	1.74
4	1.99	1.30	2.16
5	2.62	1.42	2.80
6	3.63	1.57	3.84
7	5.45	1.80	5.71
8	9.44	2.15	9.83
9	22.4	2.87	23.3
10	211	6.05	218
11	∞	∞	∞

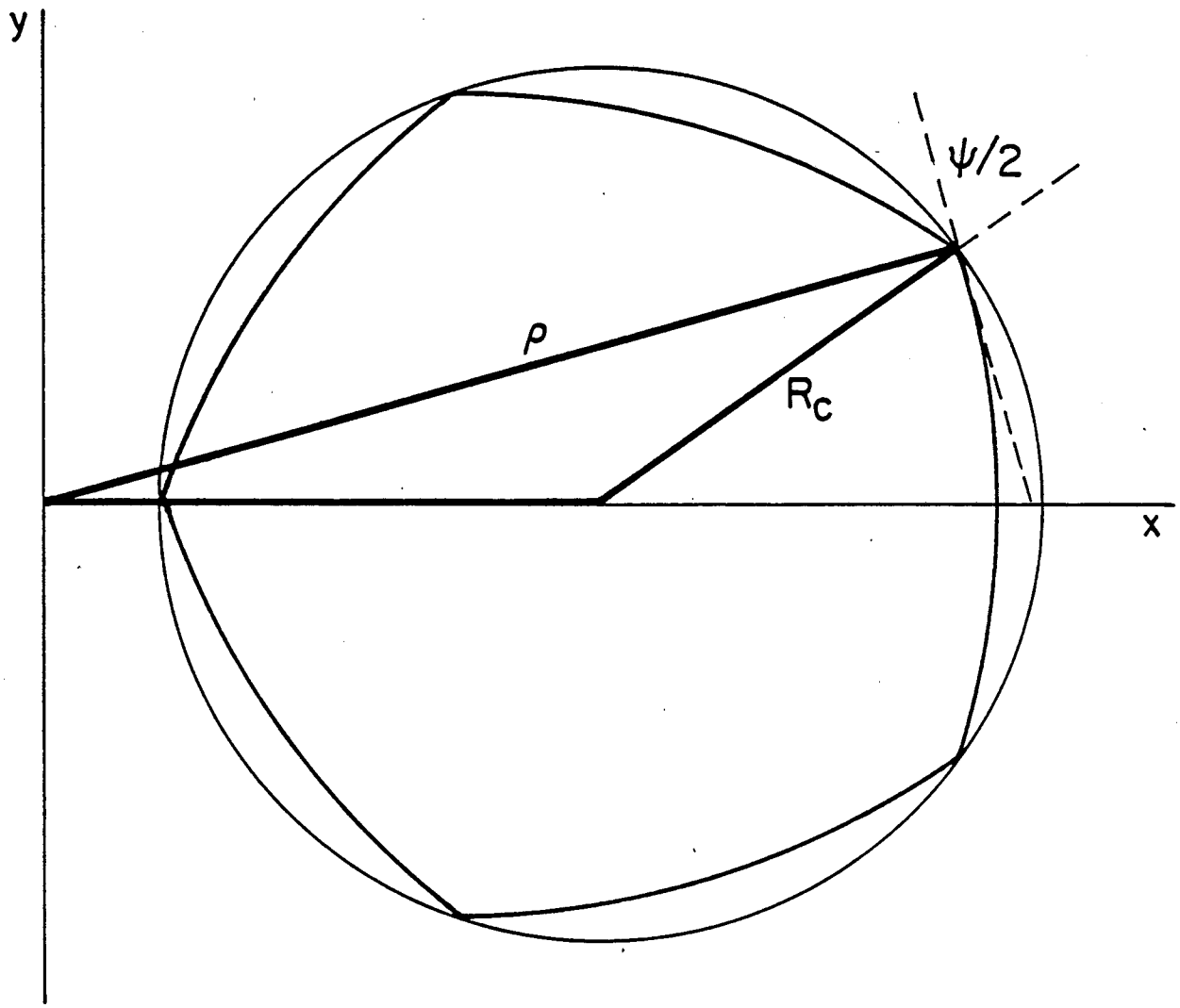

XBL 858-6519

Fig. 1

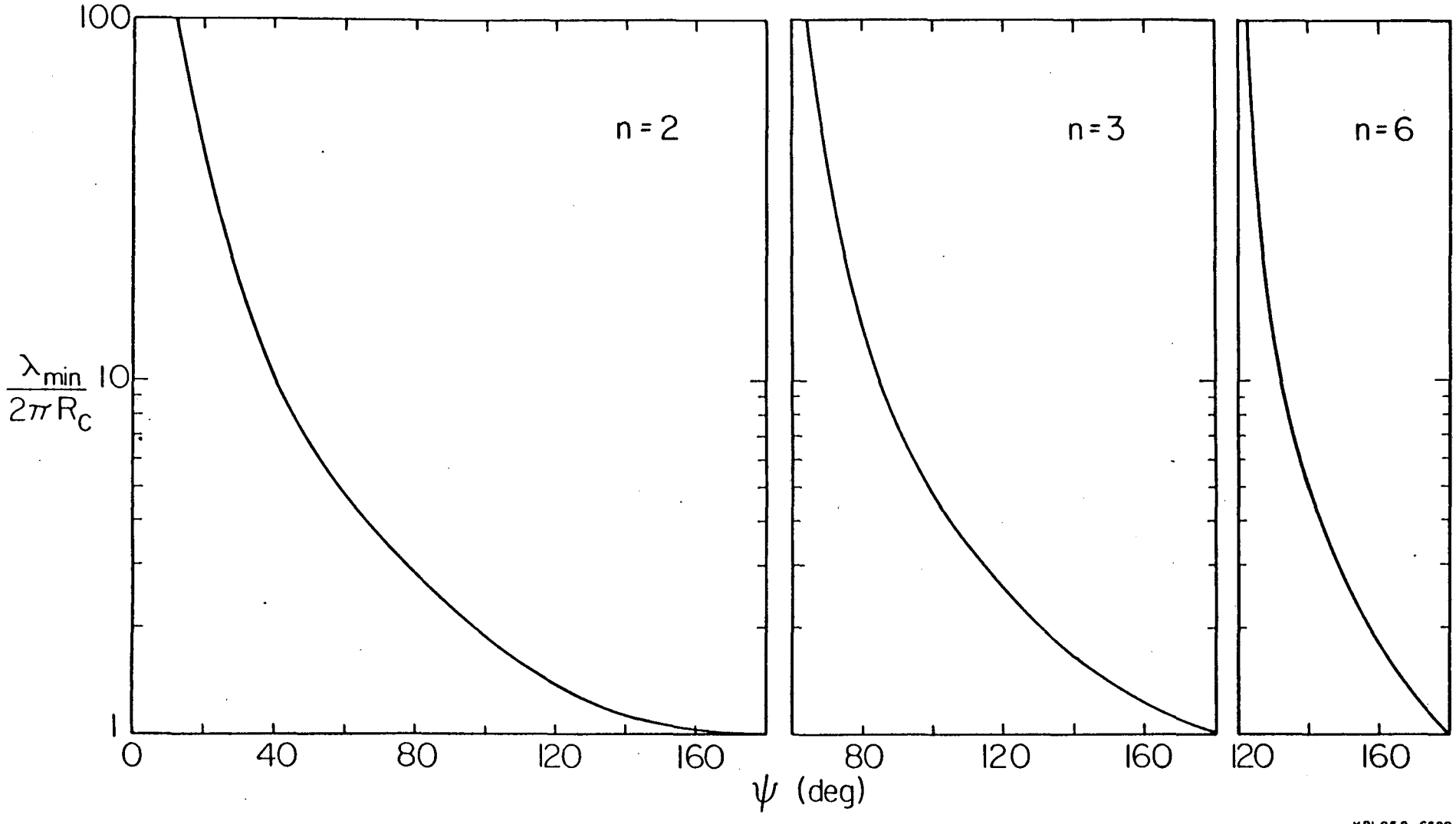
100
10
1
$\frac{\lambda_{min}}{2\pi R_c}$
n = 2
n = 3
n = 6
0
40
80
120
160
80
120
160
120
160
ψ (deg)
XBL858-6520

Fig. 2

LAWRENCE BERKELEY LABORATORY
TECHNICAL INFORMATION DEPARTMENT
UNIVERSITY OF CALIFORNIA
BERKELEY, CALIFORNIA 94720